

## Bending of Polyamide Rigid Rodlike Segments

S. M. Aharoni,\* G. R. Hatfield,<sup>†</sup> and K. P. O'Brien*Allied-Signal Inc., Engineered Materials Sector Laboratory, Morristown, New Jersey 07962.  
Received July 17, 1989; Revised Manuscript Received August 30, 1989*

**ABSTRACT:** Linear rigid rodlike polyamide macromolecules tend to orient parallel in the bulk and concentrated solution. They then respond to applied stress as an ensemble and not individually. Conversely, when isotropic gels of rigid rodlike polyamide networks are deformed, then the rodlike segments between the stiff branchpoints respond individually and bend in order to relieve the applied stress. The deformations may be external in origin, as in the case of an applied mechanical stress, or internal in origin, as in the case of network collapse due to loss of solvent from the gel. Activation energy data from the literature indicate that the preferred mechanism for chain bending in the para-aromatic polyamides is by an interconversion of anti and syn configurations, facilitated by 180° rotation around the ring-to-carbonyl bond. Each such interconversion contributes about 20 deg to the change in chain direction. Solid-state <sup>13</sup>C CP/MAS NMR spectra of the strained polyamide networks show an extra resonance downfield from the usual position of the amide carbonyl in the unstrained state. Similarly, IR spectra of strained networks show amide I peaks at frequencies higher than for the unstrained networks. These extra peaks were shown by NMR and IR not to be associated with the branchpoint residues or the nitro substitution on some of the aromatic rings. No extra peaks or shifts in peak position were observed in the spectra of the linear rigid rodlike polyamide analogues. Data generated by us and collected from the NMR and IR literature about model compounds show shifts in peak positions with strain in the same direction and of similar magnitude to the ones observed by us in the strained rigid polyamide networks.

## Introduction

Rigid rodlike polyamides and polyesters in the solid state are endowed with remarkable mechanical properties such as very high modulus and ultimate strength. They result from a strong tendency of these macromolecules to orient themselves during processing in, more or less, parallel arrays. This propensity toward orientation is manifested by the lyotropic liquid crystallinity of the polyamides and the thermotropic mesomorphicity of the polyesters. In the case of the rodlike polyamides, inter-chain hydrogen bonding between the amide groups increasingly contributes to the parallel alignment of the chains, and the system is driven to higher and higher anisotropic order as the polymer concentration increases. In the resulting highly anisotropic bulk polymer one does not find rodlike macromolecules that are individually distributed in space in a random fashion. On the contrary, in such an anisotropic bulk the chains respond to strains and stresses as an ensemble of macromolecules.<sup>1</sup> Because of this behavior such systems are of no use for the study of the stress-induced deformations (SID) of individual rodlike polyamide macromolecules.

A study of the bending of individual rodlike molecules, however, can conceivably be conducted on isotropic gels of the polymers. Such gels consist of cross-linked networks swollen with solvent, having rigid rodlike segments between rigid branchpoints, synthesized and maintained in the isotropic state. In the gel, each such rigid segment is immersed in solvent molecules, except for the rigid branchpoints and occasional contact with other segments. Segment-solvent and segment-segment hydrogen bonds (H bonds) comprise a major fraction of the interactions between the rigid segments and solvent molecules or other segments, respectively.

In the bulk and in the gelled network, polymer chain SID may be caused by externally or internally applied stress. During mechanical deformation of macroscopic samples or shrinkage of gelled polyamide rigid net-

works, the rigid segments between the stiff branchpoints may bend by torsional rotations around one or more of the three skeletal bonds between adjacent aromatic rings. The bending may be due to decreased distance between neighboring branchpoints at the end of a given segment or due to stress applied on one segment by another that is not covalently bonded to the former. We believe that such chain deformations and strain may be detected by solid-state carbon-13 NMR and infrared (IR) spectroscopy. It is well-known that when interatomic bonds are stressed, the IR bands associated with vibrations in the bond direction shift to lower frequencies while the bands associated with vibrations perpendicular to the stressed bond direction are hardly affected.<sup>2-4</sup> To the best of our knowledge, no such effects were recorded specifically involving the aromatic amide group. Therefore, we elected to follow the C=O stretch (amide I) and the amide N-H stretch bands that involve little, if any, backbone bond contribution.<sup>5</sup> Thus, in the IR investigation below we shall follow the strain- or stress-induced deformations (SID) of the amide group. These may include various deviations of the amide group from planarity, i.e., skewness, puckering about the nitrogen atom, changes in torque angles, etc. Such SID are observed in the case of aliphatic amides, as will be shown below, by a shift of the amide I band to higher frequencies. This shift, which is opposite to the one indicated above,<sup>2-4</sup> is most likely a consequence of the fact that most of the vibrational contributions to it are perpendicular to the stressed backbone and reflect the electronic decoupling of the carbonyl from the N-H moieties in the amide group. SID effects are expected to also be noticeable by solid-state <sup>13</sup>C NMR, which is very sensitive to slight changes in structure and conformation.<sup>6-9</sup> For this work we have elected to focus on the amide carbonyl (C=O) carbon and attempt to correlate changes in its chemical shift with SID of the rigid polyamide networks.

## Experimental Section

Gels of polyamide networks, in which the segments between the rigid branchpoints are rodlike in nature, were prepared by a single-step polycondensation using the Yamazaki pro-

\* Current address: Washington Research Center, W.R. Grace and Co., 7379 Route 32, Columbia, MD 21044.

cedure,<sup>10</sup> as described previously.<sup>11-13</sup> The average distance between branchpoints is determined by the shape and size of the monomers and the ratio of difunctional to tri- or tetrafunctional monomers in the reaction mixture. Analogous linear polyamides, as well as several model compounds, were prepared by the Yamazaki procedure from aromatic amines and the free acids or by Schotten-Baumann-type reaction from amines and the acid chlorides.

Infrared (IR) spectroscopy was performed by using a Perkin-Elmer Model 983 ratio-recording double-beam dispersive spectrophotometer under two resolution conditions: 3.0 cm<sup>-1</sup> at 1000 cm<sup>-1</sup> and 1.0 cm<sup>-1</sup> at 1000 cm<sup>-1</sup>. The spectral deconvolution was performed by using a dedicated Perkin-Elmer Model 7500 computer with Perkin-Elmer "CDS 3 Enhance" software. The final values of 10 cm<sup>-1</sup> half bandwidth with a 2 enhancement factor were chosen after interactive display procedures. All samples were analyzed in a KBr pellet matrix. The samples were gently ground with KBr powder, avoiding excessive shear and stress. They were then pelletized and the pellets dried under flowing liquid-nitrogen boiloff gas stream. Samples used for the determination of hydrogen bonding were then dried at 100 °C under 220 Torr for 16 h and finally transferred hot to a flowing nitrogen dry spectrophotometer to cool. Several samples were also analyzed as mineral oil mulls and as highly concentrated solutions (25 wt/vol % and higher) and mulls in DMAc, all between KBr plates.

Solid-state carbon-13 NMR spectra were obtained at 75.3 MHz on a Chemagnetics CMX300 NMR spectrometer using standard cross-polarization (CP) and magic angle spinning (MAS) techniques.<sup>14-16</sup> The magic angle was adjusted to within 0.1° by using the <sup>79</sup>Br spectrum of KBr.<sup>17</sup> CP/MAS spectra were acquired by using pulse delays of 2–60 s and contact times of 1.5–2 ms. Dipolar dephasing experiments<sup>18</sup> were often carried out to aid in spectral interpretations. Spectral deconvolutions were performed on all spectra shown below in Figures 2 and 4. They were limited to the range of 155–200 ppm, where the carbonyl carbon resonances reside. The deconvolutions were performed using NMR-1 software by New Methods Research Co. and a Du Pont Model 310 curve resolver instrument. In both cases Gaussian line-shape functions were used. The results obtained by both techniques were in satisfactory agreement. Most of the solid-state NMR spectra acquired 2500–5500 scans, resulting in somewhat noisy base line. The same level of noise appeared, of course, in the experimental and difference curves of the deconvolutions graphic displays, rendering them less than desirable for publication. In one case, however, the deconvolution was performed on a spectrum obtained from over 25 000 scans, producing smooth experimental and difference curves. This will be shown in Figure 3 below.

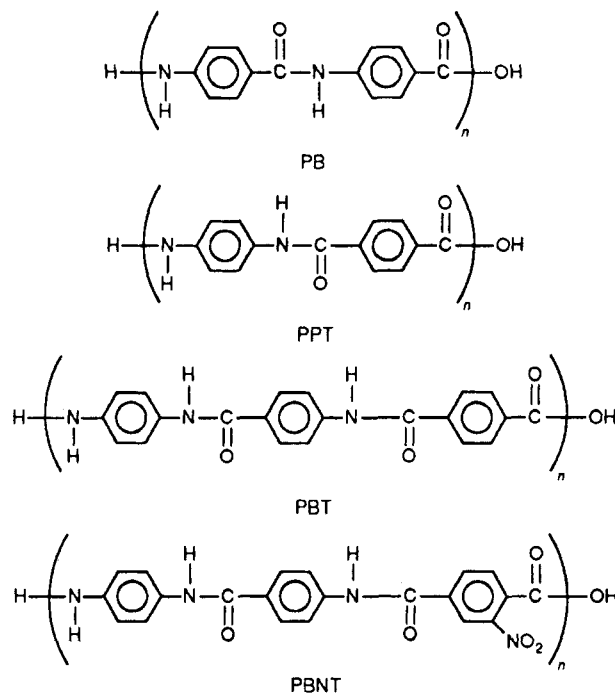
Solutions of ca. 10% sample in deuterated solvents such as DMSO, DMAc, and DMF were used to obtain <sup>1</sup>H and <sup>13</sup>C NMR spectra in order to confirm the structure and purity of the synthesized polymers, monomers, and model compounds. The solution-state NMR spectra were obtained at 50.3 and 100.6 MHz on Varian XL-200 and Varian XL-400 Fourier transform NMR spectrometers, respectively. All NMR spectra were either internally or externally referenced relative to TMS.

Wide-angle X-ray diffraction (WAXD) patterns were obtained from several gels, several dried cross-linked network polymers, some linear polymeric analogues, and a few model compounds, using a Philips APD 3600 automated diffractometer operating in parafocus mode and using monochromatized copper K $\alpha$  radiation. From the WAXD patterns of the above, the respective crystallinity indices were estimated by state of the art profile fitting procedures. Specific gravities of dried networks and linear analogues were determined by pycnometry, using mixtures of the nonsolvents carbon tetrachloride and hexanes. Dilute solution viscosities were measured at 25 °C in internal dilution Cannon-Ubbelohde glass viscometers with solvent efflux times longer than 100 s. The preferred solvent for these measurements was concentrated sulfuric acid.

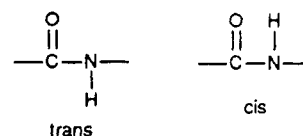
## Background

Since the focus of this work is the bending of rigid rodlike polyamides, it is important to consider the variety of polymeric structural and dynamic influences that

may play a role in the chain deformation. In addition, it is necessary to consider the nature of these polymers in their gelled state. For this work the linear<sup>19</sup> and the gelled rigid network<sup>11-13</sup> forms were prepared of the aromatic rigid rodlike polyamides poly(*p*-benzamide) (PB), poly(*p*-phenylene terephthalamide) (PPT), poly(*p*-benzanilide terephthalamide) (PBT), and poly(*p*-benzanilide nitroterephthalamide) (PBNT).

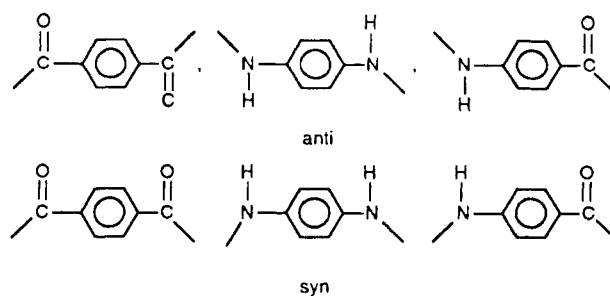


**Polymer Structure.** There exists a substantial similarity in the structure of the above polyamides. In all four, the amide group is present in a planar trans conformation:



At equilibrium in either a solution or crystalline solid state, no measurable amounts of the amide cis conformer have ever been reported. It is possible that the amide group ortho to the NO<sub>2</sub> moiety in PBNT may be somewhat skewed out of planarity, but no proof of this currently exists. Crystallographic studies reveal<sup>19-22</sup> that, with the possible exception of the nitroterephthalamide group, the aromatic rings in PB, PPT, PBT, and PBNT define planes at about  $\pm 30^\circ$  relative to the plane defined by the planar amide groups.

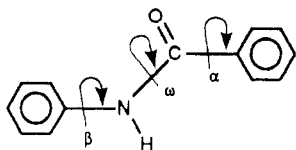
In the aromatic polyamide chains, the groups on both sides of each phenylene ring can adopt either an anti or syn configuration:



Hummel and Flory<sup>23</sup> have shown that the difference in dipole-dipole interactions between the anti and syn configurations of the diamides is only roughly 0.3 kcal/mol. This slight preference of anti over syn is about half the magnitude of  $RT$  at room temperature ( $RT \approx 0.6$  kcal/mol). As a result, crystalline PB exists in the fully syn configuration while PPT exists in the fully anti structure.<sup>22</sup> A similar situation exists for the terephthaloyl residue of diesters, for which the population of anti and syn has been shown<sup>24</sup> to be roughly equal.

The strain-free bond angles in the phenylene rings are accepted to be  $120^\circ$ . In their strain-free state, the skeletal bond angles of the amide groups slightly deviate from  $120^\circ$ : the Ar-N-C(O) angle is  $125^\circ$  and the Ar-C(O)-N angle is very close to  $117^\circ$ .<sup>5,22</sup> Because of the inequality of the amide group skeletal bond angles and the fact that their average is a little over  $120^\circ$ ,<sup>23,25</sup> a slight curvature is imparted to the polyamide chain.<sup>26</sup> This is the case independent of whether it is fully anti or fully syn. The low curvature of the rodlike polyamide chains is reflected in a large persistence length of the order of hundreds of angstroms<sup>19,25-27</sup> and becomes noticeable by viscosity measurements only when the chain surpasses 10–15 aromatic rings in length.<sup>19,28</sup> The average segment length in most of the gelled networks we have studied thus far<sup>11-13</sup> is shorter than this limit. Thus, the possible minor effects of the slight chain curvature will be disregarded in this study.

The force constants for the stretching of skeletal bonds and their bending (i.e., changing the angle between two adjoining bonds) are substantially higher<sup>5,22</sup> than the force constants involved with torsional movements around the three skeletal amide bonds:



Thus, the possible effects of skeletal bond stretching and valence angle changes will also be neglected in this study. Instead, we have chosen to concentrate on changes in dihedral angles that are presumably a dominant force in aromatic polyamide chain bending.

**The Gelled State.** When the solvent quality in gels of these networks is gradually changed, the gel swells or collapses to a new equilibrium volume with no apparent gross failure such as crack or void formation.<sup>13</sup> The degree of volume change is directly dependent on the length,  $l_0$ , of the rigid segments between branchpoints. In addition, reversible volume changes of up to 300% can occur provided the gels are allowed sufficient time to change and the incremental changes in solvent quality are small. Typically, such cycles were found to take 4–6 months. More rapid changes result in network failure. The stability of the networks in the gels was demonstrated by the constancy of the modulus<sup>13</sup> measured before and after such swelling/collapsing cycles. The best performing networks in this respect were those formed from PBNT.

Optical observations and measurements of modulus on specimens cut along three perpendicular directions indicated that all of the studied gels<sup>13,29</sup> were fully isotropic. The gelled PBT networks were found to be fully amorphous on the basis of wide-angle X-ray diffraction (WAXD) patterns. A gradual development of low level crystallinity was found to occur with the loss of solvent and gave rise to crystalline peaks at ca. 4.34 and 3.91 Å. When

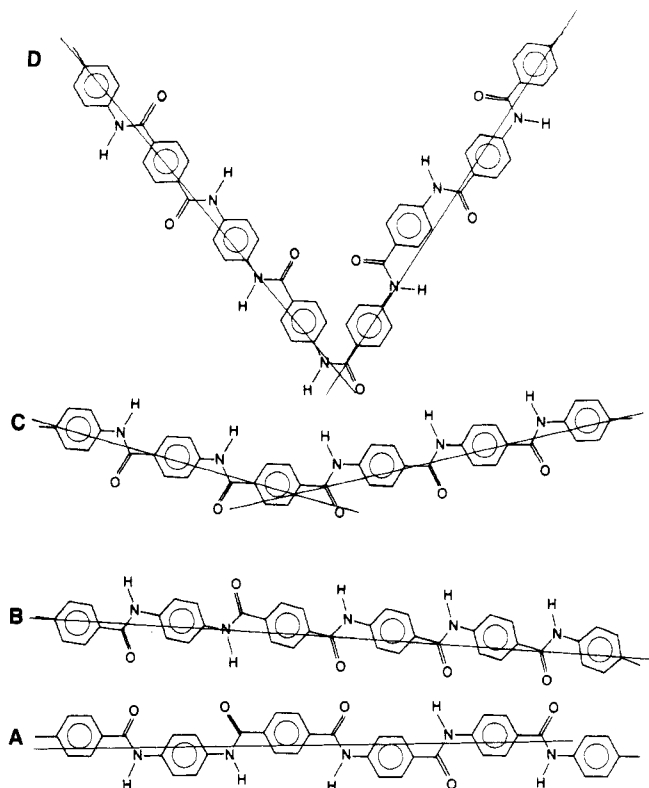


**Figure 1.** Rigid rodlike aromatic polyamides: A, fully syn configuration; B, fully anti configuration; C, a single syn conformer in an otherwise fully anti chain; D, a single cis amide in a chain of trans-amide conformers.

fully dried, the PBT networks reach a level of between 5 and 39% crystallinity, directly dependent on  $l_0$ . For both PBT and PBNT in the gel state, the amorphous halo centered at ca. 4.0 Å is smooth and Gaussian in shape. When the PBNT gels gradually dried, the shape of the amorphous halo gradually deformed, reflecting the emergence of a dominant distance at 4.4 Å. Two weaker reflections at 3.6 and 3.2 Å comprising parts of the major peak also became noticeable. However, no more than 5% crystallinity as defined by X-ray procedures could be assigned to any of the PBNT networks even when fully dried. The X-ray reflections at ca. 4.4 Å are assigned by analogy with aliphatic polyamides to the distance between hydrogen-bonded chains.<sup>19-22</sup> Thus, we find that as the rigid rodlike network gels collapse, increasing amounts of segment-segment H bonds appear. The good solvent of choice for our initially equilibrated gels was *N,N*-dimethylacetamide (DMAc). The goodness of this solvent for aromatic polyamides arises from its ability to replace segment-segment H bonds by segment-solvent H bonds. In the case of network collapse, the situation is reversed: segment-solvent H bonds are replaced by segment-segment H bonds.

## Results and Discussion

**(a) Rotational Isomeric Considerations.** In parts A and B of Figure 1, examples are given of aromatic polyamides that are fully syn and fully trans, respectively. If a single conformer of the opposite kind is introduced into these, then the chain develops a bend of about  $20^\circ$  change in direction, as illustrated in Figure 1C. Alternatively, if a trans-amide group changes to the cis-amide conformer, then the chain sharply changes course by about  $120^\circ$  deg, as shown in Figure 1D. In order to evaluate around which bond the chain is most likely to rotate and thus bend, literature data were collected in Tables I–III,

**Table I**  
Activation Energy for Rotation around Central Amide Bond ( $\omega$ )

entry	system	$E_a$ , kcal/mol	ref
1	<i>N,N</i> -dimethylformamide	20.5	<i>a</i>
2	<i>N</i> - <i>o</i> -tolyl formamide	~15.6	<i>b</i>
3	<i>N</i> -methyl- <i>N</i> -benzylformamide	23.8	<i>b</i>
4	<i>N,N</i> -dimethylacetamide	~18.1	<i>a</i>
5	<i>N,N</i> -diethylacetamide	17.5	<i>b</i>
6	<i>N,N</i> -di- <i>n</i> -propylacetamide	16.9	<i>b</i>
7	4 differently substituted acrylamides	13.1–16.8	<i>c</i>
8	<i>N,N</i> -diethylbenzamide	15.5	<i>d</i>
9	<i>N,N</i> -dimethyl-2,4,6-trimethylbenzamide	23.1	<i>b</i>
10	<i>N</i> -methyl- <i>N</i> -benzyl-2,4,6-trimethylbenzamide	27.7 $\pm$ 0.3	<i>b</i>
11	<i>N</i> -methyl- <i>N</i> -benzyl- <i>o</i> -chlorobenzamide	18.8 $\pm$ 0.3	<i>e</i>
12	14 para- and meta-substituted <i>N,N</i> -dimethylbenzamides	15.6–19	<i>f</i>
13	5 para-substituted <i>N,N</i> -dimethylbenzamides	19.8–21.6	<i>g</i>
14	8 ortho-substituted <i>N,N</i> -dimethylbenzamides	16.7–21.3	<i>h</i>
15	general (thermochemically)	21.5–22.5	<i>b</i>
16	general (NMR) preferred value	18.5–20.5	<i>b</i>
17	general (theoretical calculations)	21.5; 24.2	<i>b</i>
18	general (averaged from NMR results)	20	<i>i</i>
19	general (from IR)	14	<i>j</i>
20	piperazine polyamides	18.0 $\pm$ 0.5	<i>k</i>

<sup>a</sup> Stewart, W. E.; Siddall, T. H. *Chem. Rev.* **1970**, *70*, 517.

<sup>b</sup> Robin, M. B.; Bovey, F. A.; Basch, H. In *The Chemistry of Amides*; Zabicky, J., Ed.; Interscience: London, 1970; p 1–72. <sup>c</sup> Hobson, R. F.; Reeves, L. W. *J. Magn. Reson.* **1973**, *10*, 243. <sup>d</sup> Gryff-Keller, A.; Szczecinski, P. *Org. Magn. Reson.* **1978**, *11*, 258. <sup>e</sup> Siddall, T. H.; Pye, E. L.; Stewart, W. E. *J. Phys. Chem.* **1970**, *74*, 594. <sup>f</sup> Jackman, L. M.; Kavanagh, T. E.; Haddon, R. C. *Org. Magn. Reson.* **1969**, *1*, 109. <sup>g</sup> Fong, C. W.; Lincoln, S. F.; Williams, E. H. *Aust. J. Chem.* **1978**, *31*, 2615. <sup>h</sup> Fong, C. W.; Lincoln, S. F.; Williams, E. H. *Aust. J. Chem.* **1978**, *31*, 2623. <sup>i</sup> Levitt, M.; Lifson, S. *J. Mol. Biol.* **1969**, *46*, 269. <sup>j</sup> Miyazawa, T. *Bull. Chem. Soc. Jpn.* **1961**, *34*, 691. <sup>k</sup> Miron, Y.; McGarvey, B. R.; Morawetz, H. *Macromolecules* **1969**, *2*, 154.

**Table II**  
Activation Energy for Rotation around the Aromatic Ring to Carbonyl Bond ( $\alpha$ )

entry	system	$E_a$ , kcal/mol	ref
1	benzaldehyde	6.4–6.7	<i>a–c</i>
2	<i>p</i> -methoxybenzaldehyde	~8	<i>d</i>
3	<i>N,N</i> -dimethyl- <i>p</i> -aminobenzaldehyde	~9.5	<i>d</i>
4	singly substituted benzamides	8–14	<i>e</i>
5	<i>m</i> -dinitrobenzamides	10–12	<i>e</i>
6	<i>o</i> -dimethoxybenzamides	~20	<i>e</i>
7	<i>N</i> -methyl- <i>N</i> -benzyl- <i>o</i> -chlorobenzamide	14.5	<i>f</i>

<sup>a</sup> Green, J. H. S.; Kynaston, W.; Gebbie, H. A. *Nature* **1962**, *195*, 595. <sup>b</sup> Silver, H. G.; Wood, J. L. *Trans. Faraday Soc.* **1964**, *60*, 5. <sup>c</sup> Fateley, W. G.; Harris, R. K.; Miller, F. A.; Witkowski, R. E. *Spectrochim. Acta* **1965**, *21*, 231. <sup>d</sup> Anet, F. A. L.; Ahmed, M. J. *Am. Chem. Soc.* **1964**, *86*, 119. <sup>e</sup> Stewart, W. E.; Siddall, T. H. *Chem. Rev.* **1970**, *70*, 517. <sup>f</sup> Siddall, T. H.; Pye, E. L.; Stewart, W. E. *J. Phys. Chem.* **1970**, *74*, 594.

listing the activation energy for rotation  $E_a$  around (a) the central amide bond (angle  $\omega$ ), (b) the aromatic to carbonyl bond (angle  $\alpha$ ), and (c) the aromatic to nitrogen bond (angle  $\beta$ ), respectively.

When the data in Tables I–III are considered together, one finds that  $E_a$  is very high in all instances where an ortho-disubstituted aromatic ring is attached to the amide group from either side. When the ring is monosubstituted in the ortho position, or mono- or disubstituted in the meta and para positions, the barriers to rotation around

**Table III**  
Activation Energy for Rotation around the Aromatic Ring to Nitrogen Bond ( $\beta$ )

entry	system	$E_a$ , kcal/mol	ref
1	<i>N,N</i> -dialkyl alkylamides	~10	<i>a</i>
2	cyclic amide	~17.3	<i>a</i>
3	15 substituted anilides	~14.8 to ~22.4	<i>b</i>
4	4 ortho-substituted anilides, in ureas	~14.3 to ~17.8	$\beta$
5	2 anilides, disubstituted on ortho positions	30; 33	<i>b</i>

<sup>a</sup> Robin, M. B.; Bovey, F. A.; Basch, H. In *The Chemistry of Amides*; Zabicky, J., Ed.; Interscience: London, 1970; pp 1–72. <sup>b</sup> Stewart, W. E.; Siddall, T. H. *Chem. Rev.* **1970**, *70*, 517.

any of the three skeletal amide bonds are greatly reduced. Among the ortho-disubstituted amides, the activation energy for rotation about  $\omega$  and  $\beta$  is roughly 25–35 kcal/mol. The value of  $E_a$  for rotation about  $\alpha$ , however, is only 20 kcal/mol. Disregarding the ortho-disubstituted listings, one finds in aromatic amides that  $E_a$  for rotation about  $\omega$  tends to cluster around 18.5–20.5 kcal/mol while  $E_a$  for rotation about  $\beta$  is typically 14 to 22 kcal/mol and 6 to 14 kcal/mol for rotation about  $\alpha$ . Since all these activation energies are lower than half the height of the energy barrier for rotation around double bonds,<sup>30</sup> it is safe to assume that the double-bond character is rather small even for the central amide bond.

In comparing these data, then, it is obvious that the rotation about  $\alpha$  is greatly preferred over the rotation around the other two amide skeletal bonds. In fact, according to Arrhenius equation ( $k = Ae^{-E_a/RT}$ ), the rate constant for rotation about  $\alpha$  is roughly  $10^6$  times greater than for the other two bonds. It is interesting to note that the value of  $E_a$  for rotation about  $\omega$  and  $\beta$  span overlapping ranges, implying no major preference for rotation around either of the C(O)–N and C–N bonds.

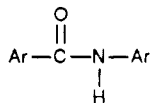
Thus, when an aromatic polyamide rigid rodlike segment in a network experiences stress in a direction normal to its axial direction, this stress is expected to be wholly or partly relieved by a rotation around the C–C(O) bond. Such a rotation may convert a configuration about a given phenylene group from anti to syn or from syn to anti. By so doing, an angle of ca. 20° appears in the segmental direction. If such a bend is insufficient to relieve all the stress, then either additional rotations of the  $\alpha$  angle or rotations of the  $\beta$  angle or  $\omega$  angle may be necessary. Very recent calculations by Coulter and Windle on aromatic polyesters<sup>31</sup> indicate a rotational barrier around the C–C(O) bond of less than 3 kcal/mol. The results of Bicerano and Clark<sup>32</sup> of 6.7 kcal/mol are closer to the experimental range. Both these results strongly support our contention that in the case of aromatic polyamides, the preferred stress-relieving bond rotation is around the C–C(O) bond.

In the crystalline state, the terephthaloyl residue of poly(ethylene terephthalate) (PET) exists in the anti form.<sup>24</sup> However, in the solution and amorphous states of both PET<sup>33,34</sup> and many model compounds,<sup>35–37</sup> the residues are present in both anti and syn forms. The minima of the energy wells associated with these conformations were shown to be essentially equal, leading to equal populations.<sup>33,34</sup> This is due to the independence of the placements of successive repeating units along the chain. This independence is guaranteed by the coplanarity of the carbonyl groups with the aromatic rings and the length of the span of the terephthaloyl residue between its two carbonyls.<sup>33</sup> A similar situation is likely to exist in the noncrystalline states of the aromatic polyamides

PB, PPT, and PBT, where the dihedral angle between the plane of the amide group and the planes of the adjoining aromatic rings is about  $\pm 30^\circ$ .<sup>20,22,38-40</sup> Evidence for this is the fact that the placement of the groups bracketing each ring is anti in the case of PPT and syn in the case of PB<sup>22</sup> and that the energetic difference between the configurations is only about 0.3 kcal/mol.<sup>23</sup> Therefore, once the rotational barriers between the anti and syn configurations are surmounted, very little, if any preference exists for one form over the other. Thus, despite the overall chain rigidity, torsional rotations are expected to impart randomness transverse to the chain backbone.<sup>23,26</sup> We believe that, because of the similarity in backbone rigidity of PBNT<sup>19</sup> and PBT, PB, and PPT,<sup>27</sup> the above arguments carry over to the case of PBNT. This is congruent with the results listed by Stewart and Siddall<sup>41,42</sup> reflecting the fact that single ortho substitutions do not greatly affect the barrier to rotation around the C-C(O) bond.

We now turn from a consideration of syn/anti rotation to cis/trans effects. It has been demonstrated<sup>43,44</sup> that the height of the rotational barrier between cis and trans amide is of the order of 20 kcal/mol. The difference between the planar cis and planar trans conformations is not higher than 2 kcal/mol,<sup>43</sup> however. NMR studies show that benzanilide exists exclusively in the trans conformation down to 253 K.<sup>45,46</sup> In our laboratory 4,4'-diaminobenzanilide (DABA) in deuterated acetone was lowered to 193 K without showing even a hint of another <sup>13</sup>C NMR resonance, or of any shift in the position of the C=O resonance. In light of the above, the indication is that in the noncrystalline linear or network aromatic polyamides the trans amide conformation is dominant, even though both cis and trans conformers are possible, and interconversion between the two conformations is of very low probability. This further indicates that the anti/syn interconversions will be favored under applied stress, possibly together with some amide deformation out of the respective planar state of equilibrium. A single ortho substituent on the aromatic ring will, most likely, not affect the expected behavior significantly.

**(b) Examination by NMR Spectroscopy.** Solid-state <sup>13</sup>C NMR spectra were obtained from bone-dry networks of PBNT and PBT and their linear analogues. In addition, 1:1 mixtures (by weight) of these systems with DMAc were also examined. The results are given in Figures 2 and 3. Since the focus of this work is changes in the



moieties, we will limit our discussion to changes observed in the carbonyl resonances at roughly 165 ppm. It is interesting to note, however, that the aromatic resonances in the swollen systems are narrower than the corresponding peaks in the bone-dry polymers. This presumably arises from motional modulation of the chemical shift dispersion induced by the presence of the solvent molecules.

Consider, first, the spectra of the various PBNT forms given in Figure 2. The carbonyl resonance in the linear form is symmetric about 165.5 ppm with a line width of 479 Hz. However, the same resonance in the network is asymmetric, with a downfield shoulder at roughly 172 ppm. In addition, the line width of the network car-

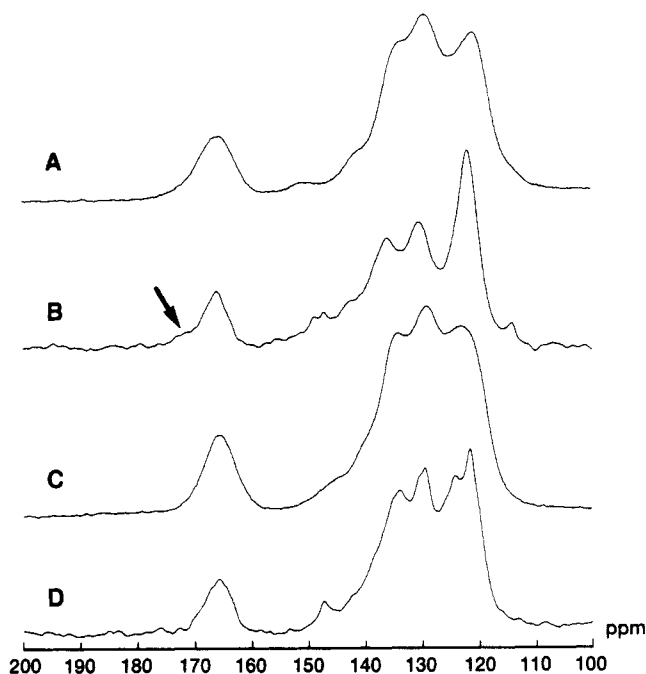


**Figure 2.** Solid-state <sup>13</sup>C CP/MAS NMR spectra: A, bone-dry PBNT network; B, PBNT network/DMAc mixture (1:1 by weight); C, bone-dry linear PBNT; D, linear PBNT/DMAc mixture (1:1 by weight).

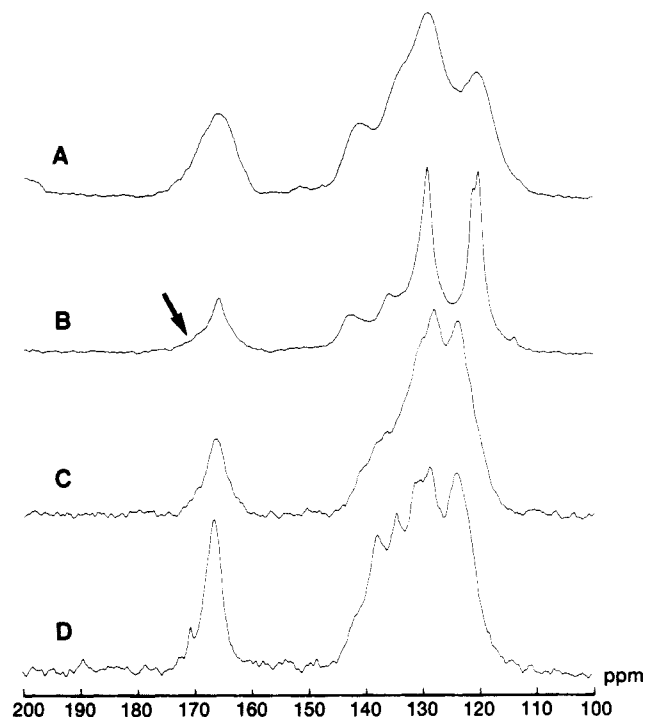


**Figure 3.** Solid-state <sup>13</sup>C CP/MAS NMR spectra: A, bone-dry PBT network; B, PBT network/DMAc mixture (1:1 by weight); C, bone-dry linear PBT; D, linear PBT/DMAc mixture (1:1 by weight).

bonyl peak has increased to 557 Hz. Spectral deconvolutions indicate that the area under the 172 ppm peak amounts to 15% of the total area of the carbonyl envelope. When DMAc is added to the two PBNT polymers, the primary resonance at 165.5 ppm sharpens while the secondary resonance at 172 ppm for the network carbonyl (indicated by an arrow) slightly enhances to ca. 19% of the total area under the carbonyl peaks. A different preparation of network PBNT and its 1:1 mixture with DMAc indicated a major carbonyl carbon resonance at 166 ppm and a minor one at 171.5 ppm. A sam-

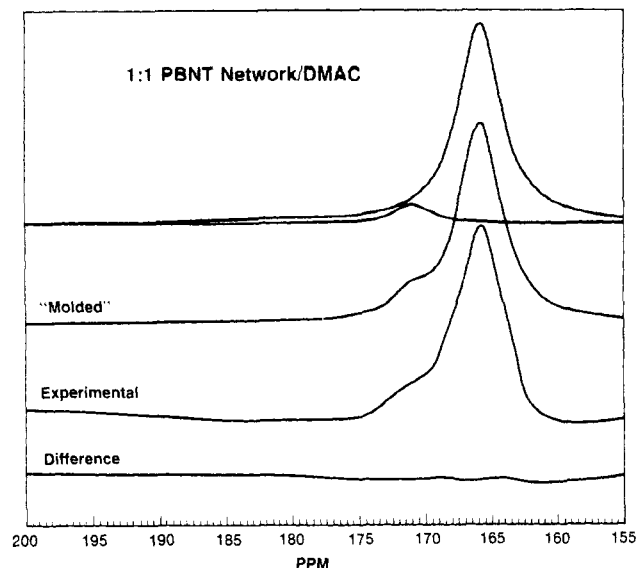


**Figure 4.** Spectral deconvolution of the carbonyl carbon region of 1:1 PBNT network/DMAc system scanned over 25 000 times. Top: two separate Gaussian contribution. "Molded" curve is their mathematical synthesis. Experimental is the spectrometer result, and difference is the subtraction of experimental from "molded" curves.

ple of this network PBNT/DMAc mixture was scanned 25 000 times and then deconvoluted (in Figure 4) to yield a minor carbonyl resonance comprising 8% of the total carbonyl in the network polymer.

The situation for the analogous PBT systems (Figure 3) is not as pronounced. The line width of the carbonyl peak in the linear system is 317 Hz while the corresponding peak in the network has a 581-Hz line width. Visual inspection of Figure 3 reveals the carbonyl peak in both systems to be more symmetric than was the case for PBNT. However, spectral deconvolutions again show that in addition to the major resonance at 165 ppm, the network carbonyl envelope contains a resonance centered at ca. 172 ppm amounting to 8% of the total carbonyl area in the case of dry network and 23% of the area for the 1:1 PBT network/DMAc system.

It is interesting to note that the carbonyl peak of the linear PBT polymer, in Figure 3C, appears as a composite peak containing a sharp and a broad resonance. Deconvolution confirmed that both peaks are centered around 165 ppm and that the sharp peak amounted to 80% of the total area while the broad peak was responsible for the rest. This system was found to be roughly 55% crystalline in the dry state and 35% crystalline in the DMAc mixture. This composite type line shape may be indicative of the semicrystalline nature of the system, with the sharp peak arising from crystalline-type carbonyls (with limited conformational distributions) and the broad peak from amorphous-type carbonyls (with more extensive conformational distributions). This type of NMR behavior has been observed in many polymers.<sup>6,7,9</sup> The other polymeric systems studied here do not show this composite type peak and were shown by X-ray techniques to be totally amorphous.

A small DMAc resonance at 170.5 ppm is evident in spectrum D of Figure 3. Deconvolution indicates a 4% contribution at identical position in spectrum D of Figure 2, belonging to the linear PBNT/DMAc mixture. No such resonance and no contribution to the shape of the peak are evident in the spectra of the network PBT/DMAc mixture, in Figure 3B, or the network PBNT/DMAc mixture in Figure 2B. We therefore conclude that

**Table IV**  
Solution-State  $^{13}\text{C}$  NMR Peak Positions (ppm) of Carbonyl Carbon<sup>a</sup>

entry	compound	peak position
1	benzanilide	165.8
2	4,4'-diaminobenzanilide	164.6
3	<i>m</i> -nitrobenzanilide	163.3
4	<i>N</i> -1-naphthylbenzamide	166.5
5	methyl benzoate	166.8
6	methyl <i>o</i> -nitrobenzoate	165.7
7	methyl <i>m</i> -nitrobenzoate	164.8
8	methyl 4-amino-3-methoxybenzoate	166.5
9	<i>p</i> -aminobenzoic acid	168.8
10	<i>p</i> -toluic acid	168.2
11	<i>o</i> -nitrobenzoic acid	166.4
12	<i>m</i> -nitrobenzoic acid	166.1

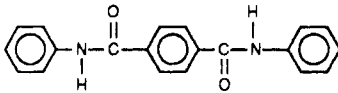
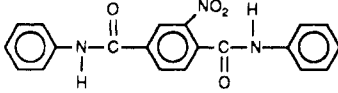
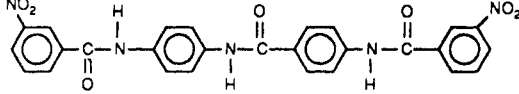
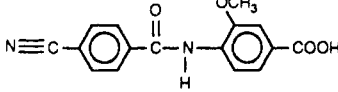
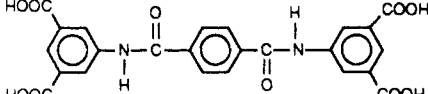
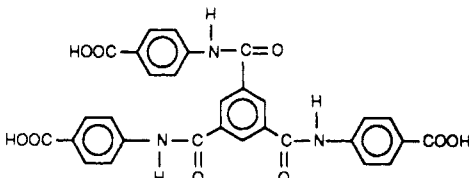
<sup>a</sup> Peak positions for entries 2 and 8 were measured in our laboratories. All other results are from carbon-13 NMR, Sadtler Research Labs., 1976-1979.

the presence of the DMAc does not affect the amide peak shape of the polymers when obtained by solid-state NMR procedures. Other potential causes for the 172 ppm region of intensity can also be eliminated. Solution-state  $^{13}\text{C}$  NMR carbonyl peak positions for several substituted and unsubstituted aromatic amides, esters, and acids are listed in Table IV. The data indicate that these substituted compounds, especially the nitro-substituted ones, produce a carbonyl carbon resonance at positions upfield from their unsubstituted analogues. Additional data, tabulated by Fong, Lincoln, and Williams<sup>47,48</sup> and by Gould and Laufer,<sup>49</sup> support our contention that the appearance of the extra downfield amide minor peak in the PBT and PBNT networks is not an inductive or steric effect of their chemical structure or their branchpoints but is the consequence of some deformation or loss of planarity in the ArC(O)N(H)Ar residue. Because carbonyl groups on both sides of a given aromatic ring are decoupled,<sup>33</sup> we believe the downfield shift of the NMR peak is not reflective of anti/syn isomeric interconversions. Importantly, the peak position of the tri- and tetrafunctional branched molecules (entries 14 and 15 in Table V) serving as models for the network branchpoints is essentially unchanged relative to the linear monomeric and polymeric analogues, and all nitro substitutions cause an upfield shift in the amide carbon peak. The molecular weight associated with each carboxyl end group in the networks was measured by titration<sup>13</sup> to be 23 500-66 700 for the PBT networks and 12 900 to 30 800 for the PBNT networks. These very high values preclude, by mere dilution, the remote possibility that the downfield peak belongs to free carboxylic acid at some chain ends.

To summarize, we believe that the downfield shift of the carbonyl peak of the PBNT and PBT dry network, which is absent in the corresponding linear analogues, reflects an undefined strain or deformation imposed on some amide residues by stresses caused by the collapsing and deforming networks during the removal of the solvent from the original gels. NMR data supporting our contention will be presented below.

In Table V are listed the polymers and various model compounds prepared for this study and the amide carbonyl peak positions obtained by solid- and solution-state  $^{13}\text{C}$  NMR. Several of the aromatic amide systems were studied by both solid-state and solution-state NMR, and it was found that in all these cases the peak positions were either identical or very close to one another. The last three entries in Table V are for model compounds, obtained from Aldrich Chemical Co., in which

**Table V**  
**Aromatic Amide Polymers and Model Compounds:  $^{13}\text{C}$  NMR Results**

entry	system	NMR peak, ppm		remarks
		carbonyl solid-state	carbonyl solutn	
1	linear PBNT, high <i>M</i>	165.5	165.3	
2	highly branched PBNT network, 45XB	165.5 + 172 sh	165.0 + 172 sh	
3	linear PBT, high <i>M</i>	166.2	166.0	
4	linear PBT, low- <i>M</i> oligomer		165.4	benzamide carbonyl terephthalamide carbonyl
5	linear PBT, low- <i>M</i> oligomer		166.2	
6	highly branched PBT network	165.0 + 172 sh		
7	3 aromatic poly(esteramides); rigid zigzags with 3-5 rings per segment		164.6, 165.0, 165.3	
8	poly(2-methoxy-5-chloro-1,4-benzamide), high <i>M</i>	162.0		
9	4,4'-diaminobenzanilide (DABA)		164.6	
10		166		
11		166 + 162		
12		166 + 163 sh		
13			164.1	
14		163		
15		165		
16	6(5 <i>H</i> )-phenanthridinone	163	160.6	Aldrich No. 29,963-4
17	2,3-dihydro-1 <i>H</i> -pyrrolo-[1,4]-benzodiazepine-5,11-dione	166 + 174	164.3 + 170.4	Aldrich No. 34,065-0
18	5,6,11,12-tetrahydrodibenzazocin-6-one	177.5	172.7	Aldrich No. 15,272-2

the amide group is increasingly strained and deformed out of the planar *cis* conformation. For the first 15 entries in the table, the amide carbonyl resonance lies between 166 and 162 ppm. In the case of PBNT and PBT networks, an additional resonance at ca. 172 ppm is evident. The shifts of the amide resonance upfield appear to be caused by electronic effects caused by various substituents on the aromatic rings. Importantly, the nitro substitution in entries 11 and 12 gives rise to an upfield resonance at about 162–163 ppm. This is in opposite direction to the secondary amide resonance in the PBNT network, appearing downfield from the major amide peak. The compounds in entries 14 and 15 serve as tetrafunctional and trifunctional branchpoints for practically all our networks. Their amide peak positions are 163 and 165 ppm, respectively. These positions are within the range of the other aromatic amides in Table V and cannot account for the secondary peaks at ca. 172 ppm evident in both networks.

The amide peak positions of entries 16, 17, and 18 in Table V reflect, we believe, the effects of deformation of the amide groups out of planarity, caused by geometrically imposed strains. The compound 6(5*H*)-phenanthridinone is remarkably flat and strain free with the two aromatic rings and the amide group all being coplanar. This was verified by computer molecular modeling as well

as by space-filling models. The compound in entry 17 is somewhat twisted about the two amide groups such that a low level of nonplanarity is present within each amide group. The 5,6,11,12-tetrahydrodibenzazocin-6-one (entry 18) is remarkably twisted with the planes of both aromatic rings in an acute angle to each other. The amide group is strongly strained and substantially nonplanar. The amide solid-state peak positions shift downfield with increased nonplanarity from 163 ppm for entry 16 through 166 ppm for entry 17 to 177.5 ppm for the highly twisted entry 18. The solution NMR amide peak shows the same shift pattern. Note that in these three compounds the amide group is in the *cis* (or *cisoid*) conformation, and yet, in the absence of deformation out of planarity, the amide peak position is within the range of aromatic amides in the *trans* conformation.

The same downfield carbonyl shift correlation with increasing strain of the amide also appears in aliphatic systems and some pertinent solution  $^{13}\text{C}$  NMR data are given in Table VI. Disregarding 2-azetidinone which is anomalous<sup>50</sup> and is included only for completeness, we find among the *cis* cyclolactams that the strained rings with five, seven, eight, and nine members give a downfield shift relative to the unstrained six-member ring. The magnitude of the downfield shift seems to correlate with the ring strain. A similar increase in downfield shift can

**Table VI**  
**Solution-State  $^{13}\text{C}$  NMR Peak Positions of Aliphatic Amides Carbonyl Resonances**

entry	compd	n-member ring	conformatn	ppm	ref
1	2-azetidinone	4	cis	168.9, 169.6	TW, <sup>a</sup>
2	2-pyrrolidone	5	cis	178.2, 179.4	a,b
3	5,5-dimethyl-2-pyrrolidone	5	cis	179.8, 179.8	c,d
4	$\delta$ -valerolactam	6	cis	177.5, 179.5	c,e
				171.2, 172.5	b,c
5	2-methylpiperid-2-one	6	cis	173.1, 173.1	d,TW
6	$\epsilon$ -caprolactam	7	cis	173.0	c
				177.9, 179.4	b,c
				179.9, 179.9	d,TW
7	1-aza-2-cyclooctanone	8	cis	178.3	b
8a	1-aza-2-cyclononanone	9	cis	177.5	b
8b	1-aza-2-cyclononanone	9	trans	175.9	b
9	lauro lactam	13	trans	174.1	b
10	6-azabicyclo[3.2.1]octan-7-one	5	cis	180.9, 181.0	c,e
11	2-azabicyclo[2.2.2]octan-3-one	6	cis	178.3, 178.8	c,d
12	3,3-diethyl-2,4(1 <i>H</i> ,3 <i>H</i> )-pyridinedione	6	cis	178.4	f
13a	2-(allylimino)-4-oxo-5-thiazolidineacet- p-anisidine (amide in ring)	5	cis	180.3	f
13b	2-(allylimino)-4-oxo-5-thiazolidineaceto- p-anisidine (amide out of ring)	5	trans	168.1	f

<sup>a</sup> TW = this work. 2-Azetidinone behaves anomalously and is given for the sake of completeness. Solid-state NMR peaks at 172.0 and 130.1 ppm reflect the anomalous behavior. Solution data were also obtained by: Lambert, J. B.; Wharry, S. M.; Block, E.; Bazzi, A. A. *J. Org. Chem.* **1983**, *48*, 3982. <sup>b</sup> Williamson, K. L.; Roberts, J. D. *J. Am. Chem. Soc.* **1976**, *98*, 5082. <sup>c</sup> Barfield, M.; Babaqi, A. S. *Magn. Reson. Chem.* **1987**, *25*, 443. <sup>d</sup> Marchal, J. P.; Brondeau, J.; Canet, D. *Org. Magn. Reson.* **1982**, *19*, 1. <sup>e</sup> Kao, L. F.; Barfield, M. *J. Am. Chem. Soc.* **1985**, *107*, 2323. <sup>f</sup> Carbon-13 NMR, Sadtler Research Labs. 1976–1979. Spectra No. 5235C, 11396C.

be seen for trans-amide rings. Here, too, the more strained nine-member ring gives a larger downfield shift than the less strained 13-member ring. Entries 8a and 8b indicate that no significant difference exists in the NMR spectra of the trans- and cis-amide conformations, as long as they are planar.

The two bicyclo compounds in entries 10 and 11 of Table VI reflect the substantial strain present in the six-member ring and the even higher strain in the five-member ring. Here, again, the higher strain is associated with a larger downfield shift. The ring in entry 12 is semirigid by virtue of one double bond in it. The compound in entry 13 contains a highly strained five-member ring in which one member is a sulfur atom (not adjacent to the ring amide) and another is a  $>\text{C}=\text{N}-$  moiety. The high ring strain is reflected in the large downfield shift of the ring amide. The other amide in the compound is in a chain between two rings. The amide is fully relaxed and its resonance is, hence, rather high upfield. It is important to mention here that the spectra in Table VI were obtained from dilute solutions of the compounds in chloroform. This minimizes hydrogen bonding and removes possible peak shifts and confusion that may arise because of the coexistence of "free" and "hydrogen-bonded" amide groups in the same sample. Chloroform is, at best, a very weak H-bonding solvent so that its presence does not significantly affect the amide peak position.

**(c) Examination by Infrared Spectroscopy.** Infrared (IR) spectroscopy is capable of revealing the presence of skewed or strained amide groups. Such deformations are associated with a decoupling of the  $\text{C}=\text{O}$  and  $\text{N}-\text{H}$  moieties due to loss of coplanarity. The electronic decoupling is reflected in the shift of the  $\text{C}=\text{O}$  stretch band (amide I) to higher frequencies and the mixed  $\text{N}-\text{H}$  bending band (amide II) to lower frequencies. Conversely, the amide planarity allows for electron delocalization from the carbonyl double bond to the  $\text{N}-\text{C}(\text{O})$  bond, increasing the double-bond character of the latter and lowering the frequency of the amide I band. Interference with the amide II band by an aromatic ring "breathing" band in all the rigid polyamides, and by the  $\text{NO}_2$

group in PBNT, limited our concentration to the amide I band alone. At the onset of our work, it was hoped that the amide I band position would be sensitive not only to loss of planarity within the amide group but also to deformations such as puckering at the nitrogen atom or reduced carbonyl–aromatic ring conjugation due to stresses applied to the polymeric chain. To ensure that the amide I band shifts are not a simple reflection of changes in hydrogen-bond levels, the  $\text{N}-\text{H}$  stretch band was monitored and the results correlated with those of the amide I band.

Networks of PBT and PBNT and their linear analogues were dried as described above. Their IR spectra showed that in the networks there exists a significant fraction of amide groups that are not hydrogen-bonded. The ratio of this fraction was estimated from the areas under the envelope of the "free"  $\text{N}-\text{H}$  stretch at about  $3400\text{ cm}^{-1}$  and the envelope of the H-bonded  $\text{N}-\text{H}$  stretch at about  $3300\text{ cm}^{-1}$ . It was found that this ratio depends mostly on the length of the rigid segments between branchpoints and less on whether the network is PBT or PBNT. The largest fraction of "free" amide groups was about 50% of the total amide present and was found in PBT networks with the shortest segments, averaging about  $32.5\text{ \AA}$  in length. In PBNT networks with segment length of  $38.5\text{ \AA}$ , the fraction of "free" amides decreased to about 25%. The presence of the "free" amides in the rigid networks is systematically different from the comparable linear aromatic polyamides in which essentially all the amide groups appear by IR to be H-bonded. The virtual absence of "free" amide groups was found to hold even when a sizable fraction of the linear polyamides was found to be amorphous by X-ray techniques.

To demonstrate our point, compare the three spectra in Figure 5. For clarity, only the spectral sections containing the  $\text{N}-\text{H}$  stretch bands (left panels) and amide I and II bands (right panels) are shown. Figure 5A is for a highly branched PBT with an averaged distance between branchpoints ( $l_0$ ) of  $208\text{ \AA}$ . Parts B and C of Figure 5 are for similar networks but with  $l_0 = 130\text{ \AA}$  and  $l_0 = 32.5\text{ \AA}$ , respectively. In the three spectra, the amide I band peaks range from  $1645$  to  $1657\text{ cm}^{-1}$ . There are no

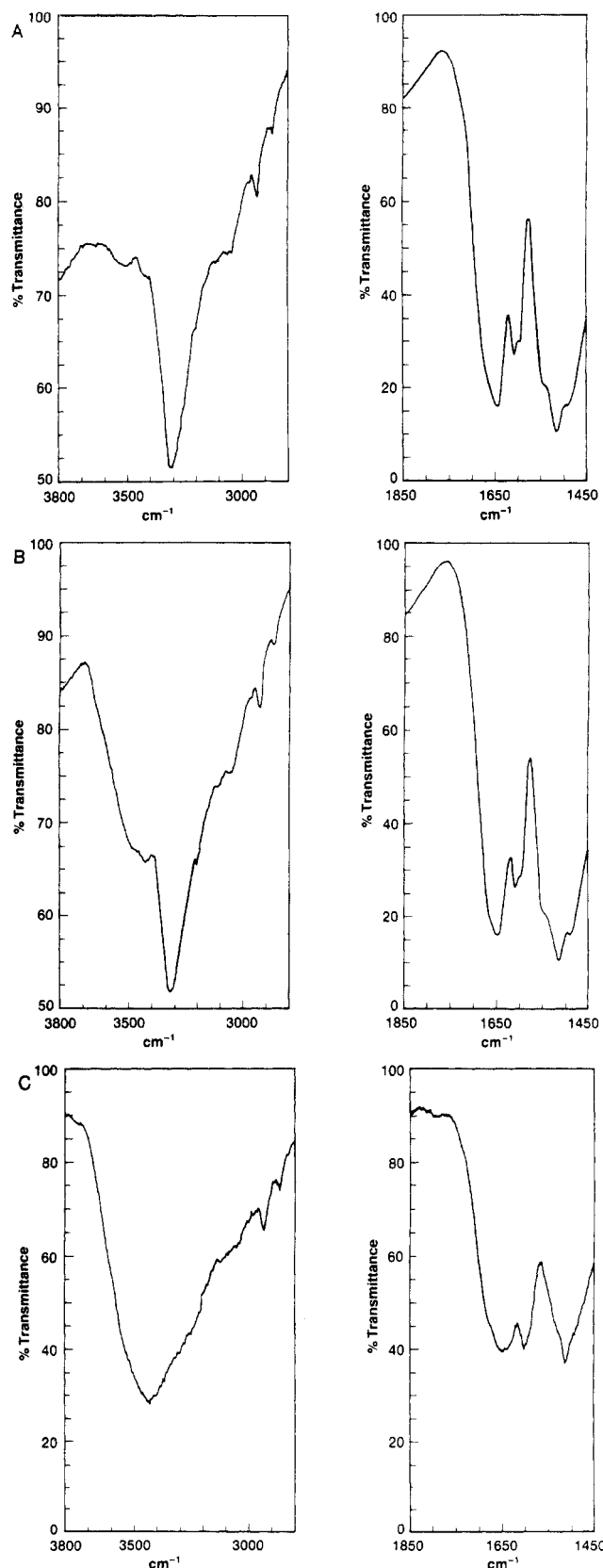


**Figure 5.** Sections of infrared spectra of bone-dry PBT network in KBr matrix: A, distance between branchpoints is 208 Å; B, 130 Å between branchpoints; C, 32.5 Å between branchpoints. Left panels are for N-H stretch bands in the region of 3500–3000  $\text{cm}^{-1}$ . These panels in A and B are twice as magnified as in C. Right panels are for regions of amide I bands at ca. 1700–1600  $\text{cm}^{-1}$  and amide II bands at 1570–1530  $\text{cm}^{-1}$ .

indications of additional amide I shoulders or peaks at frequencies higher than these. At the same time the N-H stretch region shows strong H-bonding effects. In Fig-

ure 5A the N-H envelope is dominated by a single H-bonded peak centered at 3300  $\text{cm}^{-1}$ . In Figure 5B there exists a substantial peak centered at ca. 3420  $\text{cm}^{-1}$  in addition to the peak at 3300  $\text{cm}^{-1}$ . The area under the "free" N-H stretch peak at 3420  $\text{cm}^{-1}$  was estimated by profile analysis to be not less than 20% of the area under the 3300  $\text{cm}^{-1}$  peak. In Figure 5C, the area under the "free" N-H peak at 3420  $\text{cm}^{-1}$  was estimated by the same technique to be about equal to that of the 3300  $\text{cm}^{-1}$  peak. The IR spectrum of the linear PBT is essentially identical with the spectrum in Figure 5A. A similar pattern of increasing fraction of "free" N-H stretch with shortening of  $l_0$  was previously observed<sup>51</sup> in networks of branched rigid zigzag polyamides.<sup>52</sup>

It is apparent that with the shortening of the rigid segments, an increasing fraction of the amide groups is sterically prevented from participating in hydrogen bond formation. At the same time, the amide I band position remains more or less permanent, indicating that in the case of the aromatic polyamides it is rather insensitive to the effects of H bonding. This point was clearly demonstrated by an additional experiment. Bone-dry linear and network PBNT were mixed with concentrated  $\text{H}_2\text{SO}_4$  in ratios of 3:1 by weight acid to polymer. Mixtures with higher polymer concentrations were too viscous to spread. After equilibrating for several days, the viscous solutions were spread between two KBr plates and the IR spectra were immediately taken. (Careful! HBr gas evolution. Use Hood.) The IR spectrum of  $\text{H}_2\text{SO}_4$  is essentially transparent from over 2000 down to about 1300  $\text{cm}^{-1}$ . The spectra of both polymers showed a strong and broad shoulder at ca. 3300  $\text{cm}^{-1}$  superimposed on a very broad and intense sulfuric acid envelope centered at about 2850  $\text{cm}^{-1}$ . As expected, this indicates that practically all the N-H in the amide groups are H-bonded. At the same time, the amide I region of the linear PBNT in  $\text{H}_2\text{SO}_4$  showed a single band at 1640  $\text{cm}^{-1}$ . The amide I region of the PBNT network in sulfuric acid is characterized by two bands, one at 1655  $\text{cm}^{-1}$  and the other at 1635  $\text{cm}^{-1}$ . In both solutions the amide II band at 1535  $\text{cm}^{-1}$  was reduced in intensity almost to the point of disappearance. This reflects the fact that the N-H moiety is protonated by the sulfuric acid. The above is indicative of the fact that the position of the amide I band in unstrained rigid aromatic polyamides (in solution and in the solid state) is not substantially affected by H bonding and appears in the range of 1657–1635  $\text{cm}^{-1}$ .

Infrared spectra of the model compounds benzanilide and 5,6,11,12-tetrahydrodibenzazocin-6-one are highly instructive in this respect. The first compound is exclusively in the trans amide conformation while the second exists in the cis conformation. The benzanilide spectrum<sup>53</sup> is dominated by a hydrogen-bonded N-H stretch band at 3344  $\text{cm}^{-1}$  and a sharp amide I peak at 1656  $\text{cm}^{-1}$ . The 5,6,11,12-tetrahydrodibenzazocin-6-one spectrum, obtained in this work, is dominated by an intense "free" N-H stretch band at 3430  $\text{cm}^{-1}$  and a sharp amide I band at 1640  $\text{cm}^{-1}$ . This indicates that (a) the aromatic trans and cis amide I bands fall in about the same spectral region and (b) the presence or absence of H-bonds may be overridden by other structural features.

Using this information, consider the rigid networks studied here. A magnified portion of the IR spectrum of a highly branched PBNT network (coded 45XB) is shown in Figure 6A. This network was prepared in a single step, and the average distance between branchpoints is 38.5 Å. We are interested in the amide I envelope only. It can be separated into three components: a peak at 1645

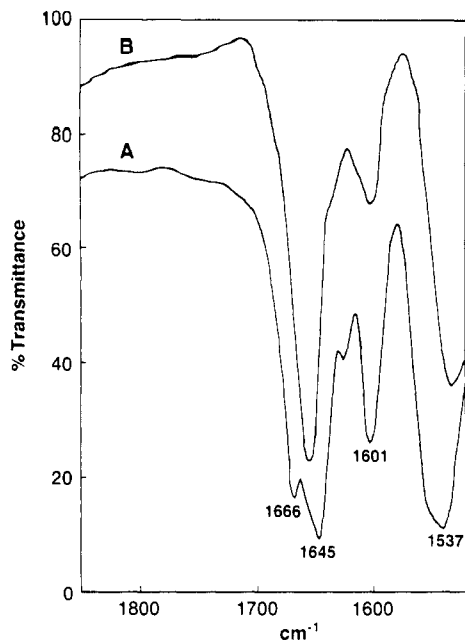


**Figure 6.** Infrared spectra of bone-dry PBNT network (A) and linear PBNT (B). Only the region of amide I and amide II is shown.

$\text{cm}^{-1}$ , a shoulder at  $1657\text{ cm}^{-1}$ , and another peak at  $1666\text{ cm}^{-1}$ . This triplet should be compared with the much narrower single band at  $1657\text{ cm}^{-1}$  observed in the spectrum of the corresponding linear PBNT, in Figure 6B, and the peak at  $1656\text{ cm}^{-1}$  observed in the spectrum of the benzanilide model compound. It is important to note that a similar tendency, expressed in increased broadening of the amide I envelope as function of decreasing segment length, is observed in the case of the PBT networks, too. The three PBT networks mentioned above show a broadening envelope with a major peak at  $1642\text{ cm}^{-1}$  and a shoulder at ca.  $1660\text{ cm}^{-1}$ . The intensity of the shoulder and its contribution to the broadening of the amide I envelope increase as  $l_0$  decreases. Conversely, the linear PBT analogue has only a single, relatively sharp, peak at ca.  $1645\text{ cm}^{-1}$ .

When the network PBNT and linear PBNT were immersed in mineral oil, the triplet in the spectrum of the former collapsed into a single peak centered at  $1657\text{ cm}^{-1}$ , as is shown in Figure 7. The linear PBNT spectrum remained unchanged with its singlet amide I band centered at  $1656\text{ cm}^{-1}$ . It should be noted that the mineral oil is a branched alkane and is incapable of participating in H-bond interactions. The dramatic change in the amide I envelope of the network PBNT indicates that the peak positions in it, especially the peak at  $1666\text{ cm}^{-1}$ , are not a simple reflection of whether the carbonyl group is H-bonded or not. Furthermore, it is unlikely that the immersion of the PBNT and PBT networks in mineral oil would permit segmental mobility to such an extent that "free" amide groups in the dry networks become H-bonded to other segmental amides in the immersed state. Conversely, we believe that in the dry networks, some of the amide groups are strained and probably skewed due to the rigid segments being bent and/or strained. This is reflected in the high-frequency peak and shoulder in the amide I envelopes of the IR spectra and in the downfield shift of the amide carbon resonance in the  $^{13}\text{C}$  NMR spectra. When mineral oil is added and fills the voids in the networks, the bent chains relax and the amide I envelopes collapse into single peaks, one at  $1657\text{ cm}^{-1}$  for the PBNT network and the other at  $1645\text{ cm}^{-1}$  for the PBT network.

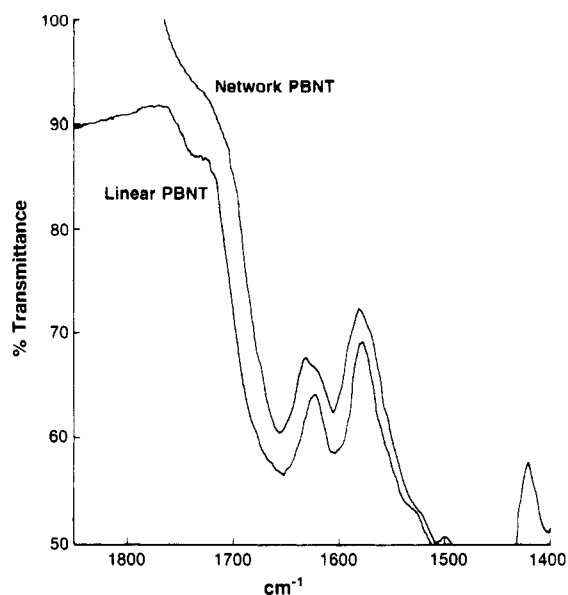


**Figure 7.** Amide I region of IR spectra of network PBNT and linear PBNT immersed in mineral oil. The amide II region is masked by the oil.

In order to ascertain the cause for the high-frequency amide I peak in the network PBNT, another experiment was performed. Fine particles of highly branched PBNT, obtained prior to gelation (characterized by  $[\eta] = 1.26\text{ dL/g}$ ;  $R_H = 120\text{ Å}$ ;  $M_w = 410\,000$ ; coded 45XB) were suspended at room temperature in DMAc in a 1:3 weight ratio PBNT/DMAc. Upon heating to  $80^\circ\text{C}$ , the network PBNT dissolved to produce an extremely viscous, optically blemishless light brown solution. This solution was allowed to equilibrate for several days, first at  $80^\circ\text{C}$  and then at ambient temperature. After an IR spectrum was obtained from the solution, the DMAc was gradually evaporated in a nitrogen stream. IR spectra were obtained from the PBNT/DMAc system at ratios of about 1:2.25, 1:1.50, and 1:1. Only the parts of the spectra where the N-H stretch and amide I and amide II bands appear are shown in Figure 8 for the 1:3 and 1:1 systems and dry PBNT network. Spectral deconvolutions were performed on the PBNT/DMAc spectra. As can be judged from the residual DMAc peak at  $1625\text{ cm}^{-1}$  in Figure 9, this was not entirely successful due to DMAc band shift caused by either DMAc-segment interactions or DMAc-DMAc interactions similar to those observed in DMF.<sup>54</sup> Nevertheless, the region of interest ( $1700\text{--}1640\text{ cm}^{-1}$ ) was left free from DMAc interference. In all cases, spectral contributions were observed that are absent in the DMAc amide region and present in the network PBNT amide I envelope. These are the three peaks centered at  $1672$ ,  $1661$ , and  $1645\text{ cm}^{-1}$  in Figure 9. A complex spectrum in the amide II region of the deconvoluted and computer "enhanced" spectrum also implies the presence of several amide forms in the PBNT network. The presence of multiple amide I peaks and the prominence among them of the  $1672\text{ cm}^{-1}$  peak, in a system largely composed of the excellent H-bonding DMAc, is a clear indication that the high-frequency peak in the amide I envelope is not due to "free" amide carbonyl but is caused by a decoupled amide, i.e., a strained amide group either deformed out of planarity or twisted around the C-C(O) bond at an angle substantially different from the relaxed state, or both.

The effects of strain on carbonyl peak position is even more obvious in the cases of cycloaliphatic ketones, lactones, and, especially, lactams. In all of these, a shift of

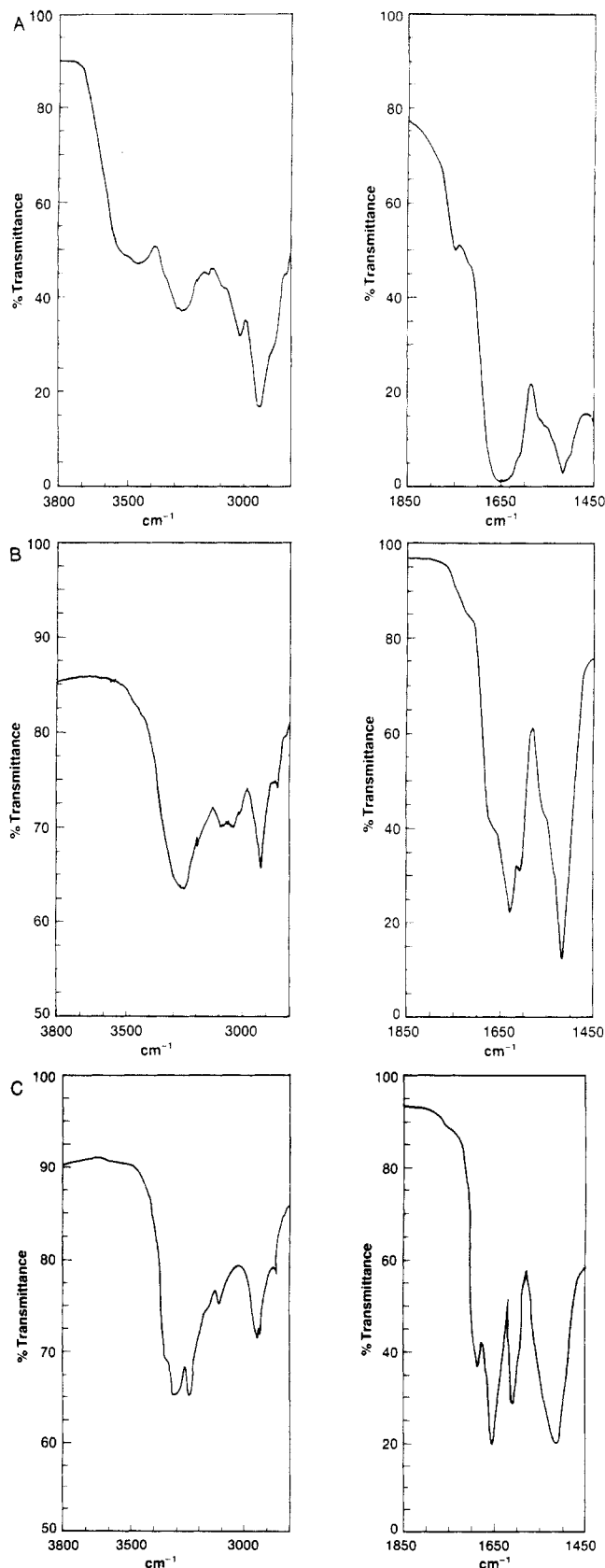


**Figure 8.** Sections of infrared spectra of the highly branched PBNT 45XB: A, 1:3 by weight network PBNT/DMAc; B, 1:1 network/DMAc; C, bone-dry PBNT network. Left panels are for N-H stretch bands, and right panels are for the amide I and amide II bands. Band at about  $3500\text{ cm}^{-1}$  in A is associated with DMAc. Left panels in B and C are twice as magnified as in A.

about  $70\text{ cm}^{-1}$  to higher frequency is evident upon decreasing the ring size from seven to four members.<sup>55</sup> Another

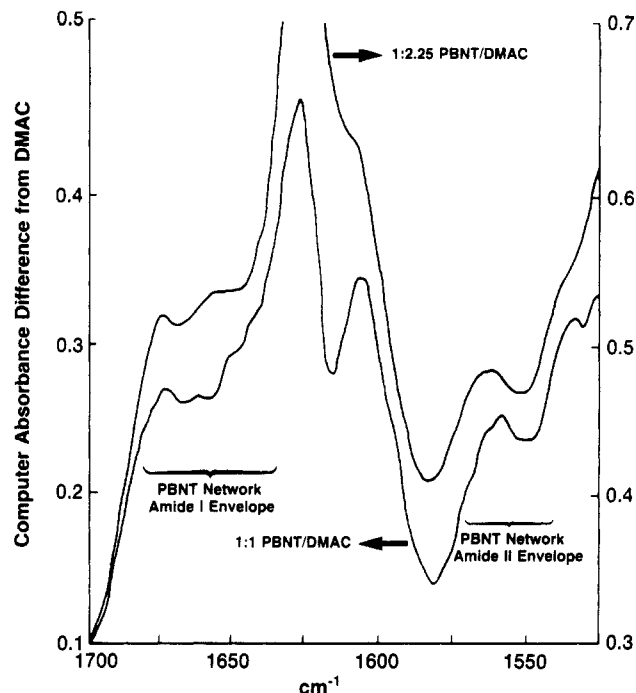


**Figure 9.** Spectral deconvolutions of the PBNT network/DMAc mixtures. The PBNT network amide I envelope between  $1700$  and  $1640\text{ cm}^{-1}$  and the amide II envelope between  $1570$  and  $1530\text{ cm}^{-1}$  are indicated.

instructive example of the effect of strain on IR band position in a series of cycloaliphatic lactams was given by Hallam and Jones.<sup>56</sup> Choosing the N-H stretch band and using very dilute solutions in  $\text{CCl}_4$  to eliminate H bonding, they show a clear trend in the band frequency, going from high frequency in the smaller rings to lower frequencies as the ring size increases. Thus, for lactams with cis amide, the frequency drops from  $3455\text{ cm}^{-1}$  for 2-pyrrolidinone to  $3397\text{ cm}^{-1}$  for the 10-member cyclolactam. The trans conformation is present in 10-member through 13-member cyclolactams. Here the change in band frequency is much smaller and yet the trend is similar. A skewed amide is present in the nine-member ring with the N-H stretch appearing at  $3442\text{ cm}^{-1}$ . Similar results were obtained by Hanai et al.<sup>57</sup> on a smaller set of cyclic lactams. In this case, the amide I band for both the "free" and H-bonded states was also followed. This is similar to our experiments. Going from the cis-amide four-member lactam to seven-member lactam, Hanai et al.<sup>57</sup> report a change in the amide I band from  $1781$  to  $1676\text{ cm}^{-1}$  in the "free" state and from  $1769$  to  $1672\text{ cm}^{-1}$  for the hydrogen-bonded form. A plot of the amide I frequency as function of ring size in Hallam and Jones<sup>56</sup> follows the same pattern for both cis and trans amides. We may conclude, hence, that changes in strains induced by changes in ring size manifest themselves in changes in the IR band positions associated with the amide group. These strains may be reflected by changes in dihedral angles around the C-C(O) or C-N bonds away from equilibrium or in deviations from strict planarity within either the cis- or the trans-amide group, as was demonstrated by Dunitz and associates<sup>43,58</sup> and Hallam and Jones.<sup>56,59</sup>

Coleman and associates<sup>60,61</sup> found that upon heating, linear aliphatic polyamides and polyurethanes IR bands in the "free" amide regions appear and their intensity increases with increased temperature at the expense of the H-bonded bands. Most of the changes occur around the respective melting point. In the case of the linear aliphatic polymers, the chain mobility is facilitated practically exclusively by trans-gauche isomeric interconver-

sions in the flexible alkylene sequences, requiring only about 3 kcal/mol to surpass the energy barrier.<sup>24,62</sup> In these polymers the amide groups are completely planar in the trans conformation. The increased chain motion with heating weakens and/or disrupts the hydrogen bonds, giving rise to amide I band at higher frequency. Such chain motions cannot take place in our rigid polymers, linear or network. In our case, enhanced chain mobility must be associated with motions of the amide skeletal bonds or around them, such as puckering at the nitrogen, skewness of the amide residue, and changes in torsional angles away from equilibrium, leading to anti/syn interconversions. Such motions apparently lead to decoupling of the  $>C=O$  from the  $>N-H$  fragments in some of the aromatic amides and a shift of some of the amide I band to higher frequency. This is independent of the presence or absence of H bonds in the system.

In light of the above, we conclude that the amide I peak position shifts observed in the dry rigid networks reflect strains imposed on these networks by their collapse from the more swollen gel state. Similar such strains are, most likely, caused by network deformation due to the application of high mechanical stresses.

One final point. The IR results indicate that the presence of high-frequency amide I band in the branched networks is structurally dependent and is most prominent in systems exhibiting the least amount of segment-segment H bonding. These are the very systems where a downfield secondary carbonyl carbon resonance appears in the solid-state NMR spectra. Furthermore, the downfield NMR peak does not appear in the case of the highly H-bonded linear polyamides in either the bulk or in high concentration solutions in strongly H-bonding solvents such as DMAc/5% LiCl or concentrated  $H_2SO_4$ . Thus, unlike several literature references such as ref 63, one may not directly relate the secondary NMR downfield peak with the presence or intensity of H bonds in the present system.

### Summary

The results described above lead us to believe that the slow removal of good solvent from the polymer gels encourages the substitution of segment-solvent H bonds by segment-segment ones. As the segment-segment H bonds increase in number, the increasing attractive interaction between neighboring segments brings them closer and closer together. This movement is, undoubtedly, associated with developing stresses within the shrinking networks. These stresses may be relieved by configurational interconversions from anti to syn, or vice versa, and/or changes of amide groups from planar to skew conformation. The relaxation of stresses during swelling may be explained by a reversal of the above process. When mechanical stress is applied to the rigid network gel, the deformation is facilitated by chain bending made possible by anti/syn interconversions and/or changes in the amide group. The stresses on the rigid segments may be relieved by such isomeric changes and, perhaps, by changes in the population of segment-solvent H bonds in favor of segment-segment H bonds. The rigid network collapse was found to be associated with the appearance of an extra downfield carbonyl peak by carbon-13 NMR and an extra amide IR peak at higher frequency than usual. No such shifts were observed here or are reported in the literature for the linear analogues of the above networks. The extra peaks in both the IR and NMR spectra were demonstrated not to belong to the tri- or tetrafunctional branchpoints and to be independent of the absence of H bonding. These peaks are also indepen-

dent of electron delocalization or induction effects of the nitro substituent in the PBNT networks. Thus, we believe these shifted peaks reflect stress-induced deformation out of planarity of some of the  $ArC(O)N(H)Ar$  groups or changes in the torsional angles away from their equilibrium positions. In light of the energy barrier data presented above, the most likely changes in the torsional angles are occasional interconversions from anti to syn, or vice versa, followed by deformation out of planarity of the amide residues. Each anti/syn interconversion contributes about 20 deg to the stress-induced change in chain direction. Because the energy barriers to such an interconversion are rather low, we believe it to be the major mode of SID of the collapsing, or swelling, networks. The isomerization of the amide residue from planar trans to planar cis may contribute 120° to the change in chain direction but requires overcoming much higher energy barriers, making it rather unlikely. Distortions of the amide group away from planarity may also contribute to the directional changes of the chain, but the magnitude and frequency of such contributions are not known to us at present. As a matter of fact, the creation of only one or two segment-segment H bonds per rodlike segment are sufficient to overcome the anti/syn interconversion energy barrier.

There are several literature treatments of chain deformation conceptually similar to ours. Among them one finds the works of Bahar and Erman<sup>62</sup> and Bleha and Gajdos<sup>64</sup> on alkylene chains and, closer to our work, the studies of Tsvetkov<sup>26</sup> and Slutsker et al.<sup>65</sup> on aromatic polyamides and Gardner et al.<sup>66</sup> on aromatic polyester. Importantly, all these studies indicate that chain deformation is facilitated by some rotational isomerization which, in turn, requires the investment of relatively small amounts of energy.

**Acknowledgment.** The help of Drs. R. Brambilla and N. S. Murthy with various aspects of the experimental work is greatly appreciated. We thank Professor S. Krimm and Dr. W. B. Hammond for many fruitful discussions.

### References and Notes

- (1) Deteresa, S. J.; Allen, S. R.; Farris, R. J.; Porter, R. S. *J. Mater. Sci.* **1984**, *19*, 57.
- (2) Vettergren, V. I.; Novak, I. I. *J. Polym. Sci., Polym. Phys. Ed.* **1973**, *11*, 2135.
- (3) Wool, R. P.; Statton, W. O. *J. Polym. Sci., Polym. Phys. Ed.* **1974**, *12*, 1575.
- (4) Friedland, K. J.; Marikhin, V. A.; Myasnikova, L. P.; Vettergren, V. I. *J. Polym. Sci., Polym. Symp.* **1977**, *58*, 185.
- (5) Kim, P. K.; Hsu, S. L.; Ishida, H. *Macromolecules* **1985**, *18*, 1905.
- (6) Fyfe, C. A. *Solid-State NMR for Chemists*; CFC Press: Guelph, 1983.
- (7) Komoroski, R. A., Ed. *High Resolution NMR Spectroscopy of Synthetic Polymers in Bulk*; VCH Publishers: Deerfield Beach, FL, 1986.
- (8) Aharoni, S. M.; Correale, S. T.; Hammond, W. B.; Hatfield, G. R.; Murthy, N. S. *Macromolecules* **1989**, *22*, 1137.
- (9) Hatfield, G. R.; Glans, J. H.; Hammond, W. B., manuscript submitted for publication.
- (10) Yamazaki, N.; Matsumoto, M.; Higashi, F. *J. Polym. Sci., Polym. Chem. Ed.* **1975**, *13*, 1373.
- (11) Aharoni, S. M. *Macromolecules* **1982**, *15*, 1311.
- (12) Aharoni, S. M.; Wertz, D. H. *J. Macromol. Sci., Phys.* **1983**, *B22*, 129.
- (13) Aharoni, S. M.; Edwards, S. F. *Macromolecules* **1989**, *22*, 3361.
- (14) Pines, A.; Gibby, M. G.; Waugh, J. S. *J. Chem. Phys.* **1973**, *59*, 569.
- (15) Schaefer, J.; Stejskal, E. O. *J. Am. Chem. Soc.* **1976**, *98*, 1031.
- (16) Schaefer, J.; Stejskal, E. O. In *Topics in Carbon-13 NMR Spectroscopy*; Levy, G. C., Ed.; Wiley: New York, 1979; Vol. 3.
- (17) Frye, J. S.; Maciel, G. E. *J. Mag. Reson.* **1982**, *48*, 125.

- (18) Opella, S. J.; Frey, M. H. *J. Am. Chem. Soc.* **1979**, *101*, 5854.
- (19) Aharoni, S. M. *Macromolecules* **1987**, *20*, 2010.
- (20) Northolt, M. G.; Van Aartsen, J. J. *J. Polym. Sci., Polym. Lett. Ed.* **1973**, *11*, 333.
- (21) Northolt, M. G. *Eur. Polymer J.* **1974**, *10*, 799.
- (22) Tashiro, K.; Kobayashi, M.; Tadokoro, H. *Macromolecules* **1977**, *10*, 413.
- (23) Hummel, J. P.; Flory, P. J. *Macromolecules* **1980**, *13*, 479.
- (24) Flory, P. J. *Statistical Mechanics of Chain Molecules*; Interscience: New York, 1969; pp 49-66, 190-192.
- (25) Erman, B.; Flory, P. J.; Hummel, J. P. *Macromolecules* **1980**, *13*, 484.
- (26) Tsvetkov, V. N. *Eur. Polym. J.* **1976**, *12*, 867.
- (27) Zero, K.; Aharoni, S. M. *Macromolecules* **1987**, *20*, 1957.
- (28) Baird, D. G.; Ballman, R. L. *J. Rheol.* **1979**, *23*, 505.
- (29) Aharoni, S. M.; Murthy, N. S.; Zero, K.; Edwards, S. F. *Macromolecules*, in press.
- (30) Volkenstein, M. V. *Configurational Statistics of Polymeric Chains*, Interscience: New York, 1963; pp 48-156, 202-210, 301-390.
- (31) Coulter, P.; Windle, A. H. *Macromolecules* **1989**, *22*, 1129.
- (32) Bicerano, J.; Clark, H. A. *Macromolecules* **1988**, *21*, 585.
- (33) Williams, A. D.; Flory, P. J. *J. Polym. Sci., Polym. Phys. Ed.* **1967**, *5*, 417.
- (34) Štokr, J.; Schneider, B.; Doskočilova, D.; Lövy, J.; Sedláček, P. *Polymer*, **1982**, *23*, 714.
- (35) Sedláček, P.; Štokr, J.; Schneider, B. *Collect. Czech. Chem. Commun.* **1981**, *46*, 1646.
- (36) Štokr, J.; Sedláček, P.; Doskočilova, D.; Schneider, B.; Lövy, J. *Collect. Czech. Chem. Commun.* **1981**, *46*, 1658.
- (37) Schneider, B.; Sedláček, P.; Doskočilova, D.; Štokr, J.; Lövy, J. *Collect. Czech. Chem. Commun.* **1981**, *46*, 1913.
- (38) Harkema, S.; Gaymans, R. J. *Acta Crystallogr.* **1977**, *B33*, 3609.
- (39) Adams, W. W.; Fratini, A. V.; Wiff, D. R. *Acta Crystallogr.* **1978**, *B34*, 954.
- (40) Harkema, S.; Gaymans, R. J.; Van Hummel, G. J.; Zylberlicht, D. *Acta Crystallogr.* **1979**, *B35*, 506.
- (41) Stewart, W. E.; Siddall, T. H. *Chem. Rev.* **1970**, *70*, 517.
- (42) Siddall, T. H.; Pye, E. L.; Stewart, W. E. *J. Phys. Chem.* **1970**, *74*, 594.
- (43) Winkler, F. K.; Dunitz, J. D. *J. Mol. Biol.* **1971**, *59*, 169.
- (44) Levitt, M.; Lifson, S. *J. Mol. Biol.* **1969**, *46*, 269.
- (45) Kessler, H.; Rieker, A. *Liebigs Ann. Chem.* **1967**, *708*, 57.
- (46) Lumley Jones, R.; Smith, R. E. *J. Mol. Struct.* **1968**, *2*, 475.
- (47) Fong, C. W.; Lincoln, S. F.; Williams, E. H. *Aust. J. Chem.* **1978**, *31*, 2615.
- (48) Fong, C. W.; Lincoln, S. F.; Williams, E. H. *Aust. J. Chem.* **1978**, *31*, 2623.
- (49) Gould, S.; Laufer, D. A. *J. Magn. Reson.* **1979**, *34*, 37.
- (50) Lambert, J. B.; Wharry, S. M.; Block, E.; Bazzi, A. A. *J. Org. Chem.* **1983**, *48*, 3982.
- (51) Aharoni, S. M., unpublished observations.
- (52) Aharoni, S. M. *Macromolecules* **1988**, *21*, 185.
- (53) Pouchert, C. J. *The Aldrich Library of FT-IR Spectra*, 1st ed.; Aldrich: Milwaukee, WI, 1985; Vol. 2, spectrum 375C.
- (54) Shelley, V. M.; Talintyre, A.; Yarwood, J.; Buchner, R. *Faraday Discuss. Chem. Soc.* **1988**, *85*, 211.
- (55) Conley, R. T. *Infrared Spectroscopy*; Allyn & Bacon: Boston, 1966; pp 140-148.
- (56) Hallam, H. E.; Jones, C. M. *J. Mol. Struct.* **1967-1968**, *1*, 413.
- (57) Hanai, K.; Maki, Y.; Kuwae, A. *Bull. Chem. Soc. Jpn.* **1985**, *58*, 1367.
- (58) Chakrabarti, P.; Dunitz, J. D. *Helv. Chim. Acta* **1982**, *65*, 1555.
- (59) Hallam, H. E.; Jones, C. M. *J. Chem. Soc. A* **1969**, 1033.
- (60) Skrovanek, D. J.; Painter, P. C.; Coleman, M. M. *Macromolecules* **1986**, *19*, 699.
- (61) Coleman, M. M.; Lee, K. H.; Skrovanek, D. J.; Painter, P. C. *Macromolecules* **1986**, *19*, 2149.
- (62) Bahar, I.; Erman, B. *Macromolecules* **1987**, *20*, 2310.
- (63) Imashiro, F.; Maeda, S.; Takegoshi, K.; Terao, T.; Saika, A. *Chem. Phys. Lett.* **1983**, *99*, 189.
- (64) Bleha, T.; Gajdos, J. *Collect. Polym. Sci.* **1988**, *266*, 405.
- (65) Slutsker, L. I.; Uteviskii, L. E.; Chereiskii, Z. Yu.; Perepelkin, K. E. *J. Polym. Sci., Polym. Symp.* **1977**, *58*, 339.
- (66) Gardner, K. H.; Gochanour, C. R.; Irwin, R. S.; Sweeny, W.; Weinberg, M. *Mol. Cryst. Liq. Cryst.* **1988**, *155*, 239.

## X-ray Diffraction and Nuclear Magnetic Resonance Studies of Nylon 6/I<sub>2</sub>/KI Complexes and Their Transformation into the $\gamma$ Crystalline Phase

N. Sanjeeva Murthy,\* Galen R. Hatfield, and Jeffrey H. Glans

*Corporate Technology, Allied-Signal, Inc., P.O. Box 1021R,  
Morristown, New Jersey 07960-1021. Received July 24, 1989;  
Revised Manuscript Received August 29, 1989*

**ABSTRACT:** Solid-state <sup>13</sup>C and <sup>15</sup>N NMR results relevant to the structure of iodinated Nylon 6 (N6) and its conversion into the  $\gamma$  phase are presented. The polymer chain-axis repeat in KI/I<sub>2</sub>-treated N6 is 15.7 Å. This is shorter than that for the  $\alpha$  (17.2 Å) and  $\gamma$  (16.8 Å) structures. This new structure gives rise to a carbonyl NMR peak at 176.5 ppm, compared to 173.4 and 173.1 ppm in the  $\alpha$  and  $\gamma$  structures, respectively. Some NMR evidence is presented that suggests that the interchain hydrogen bonds in the complex are weak or absent. Additionally, there are likely to be conformational changes in the methylene carbons adjacent to the amide moiety. Such changes may provide a mechanism by which the chain-axis shortens and is capable of forming a commensurate structure with I<sub>5</sub><sup>-</sup> ions as postulated by XRD studies. Experimental evidence is also presented that indicate that  $\gamma$  crystalline phase is formed during initial KI/I<sub>2</sub> desorption even while the amorphous chain segments remain complexed. This suggests that the  $\gamma$  phase evolves from the complex without going through an identifiable, intermediate, native amorphous phase.

### Introduction

The most thermodynamically stable crystalline structure of Nylon 6 (N6) is known as the  $\alpha$  form. In this

structure the molecules are in an extended-chain conformation with hydrogen bonds between antiparallel chains.<sup>1</sup> The other crystalline form of Nylon 6 is known as  $\gamma$ . Here, the hydrogen bonds are between parallel chains and the molecules form pleated hydrogen-bonded sheets.<sup>2</sup>

\* To whom all correspondence should be addressed.